Open Access Journal

Journal of Power Technologies 97 (1) (2017) 52–60

journal homepage:papers.itc.pw.edu.pl

LES numerical study on in–injector cavitating flow

Rafał Pyszczek[a], Łukasz Jan Kapusta[a,*], Andrzej Teodorczyk[a]

[a] *Institute of Heat Engineering, Warsaw University of Technology, Nowowiejska Street 21/25, 00-665 Warsaw, Poland*

Abstract

In this paper a computational study on hexane flow in a fuel injector is presented. Large Eddy Simulation (LES) was used to capture the turbulent patterns present in the flow. The main aim was to investigate the cavitation phenomenon and its interaction with turbulence as well as the influence of injection pressure and backpressure on fuel mass flow and flow conditions. Analysis of the approach to define the outlet boundary conditions in terms of convergence time and fluid mass outflow oscillations formed a crucial part of the study. Numerical simulations were performed with AVL Fire CFD (Computational Fluid Dynamics) software. The Euler-Euler approach and multifluid model for multiphase flow modelling were applied. Injector needle movement was included in the simulation. Results show that the additional volumes attached to the nozzle outlets improved the convergence of the simulations and reduced mass outflow oscillations. Fuel mass flow at the outlets was dependent on inlet pressure, position of the needle and backpressure, while the influence of backpressure on fuel mass flow was negligible. The presence of the vapor phase at the exit of the nozzles did not affect average fuel mass flow. All the simulations showed interaction between the gaseous phase distribution and the turbulence of the flow.

Keywords: cavitation; cavitating flow; in-injector flow; Eulerian multiphase; multiphase flow; numerical simulation; Large Eddy Simulation; LES

1. Introduction

Economic growth in the industrial sector in recent decades has been a key driver in the increase in emissions to the atmosphere. Every year, natural resources of planet Earth are shrinking and more CO_2 is released into the atmosphere. Therefore, there is a general awareness that emissions should be reduced wherever possible. The flaring of associated gas and other light hydrocarbons in the oil fields is an example of a practice that is both wasteful and polluting. The reason for that situation is the fact that many gaseous and liquid hydrocarbons resulting as by-products from industrial processes are characterized by a composition that varies over time, leaving them unsuitable for conventional energy conversion equipment. However, with the right technology, they might offer opportunities for replacing the conventional fuels used to generate electricity or mechanical drive power. At first glance, it seems that from the economic point of view, the process of converting such fuel into useful energy has to be profitable. Nevertheless, there are some requirements which need to be met. Most existing technologies are sensitive to fuel quality. Thus, any switch to 'difficult fuels' of varying composition and containing undesirable compounds may lead to a dramatic decrease in TBO (Time Between Overhaul) and an increase in operating costs, which could easily outweigh any possible profits to be made from using this kind of fuel. One possible solution is to supply the heavy-duty piston engines working directly on the oil fields with a specially designed fuel system for hydrocarbons of these types. The prospective fueling technology is a dual-fuel direct injection system where the second fuel will provide reliable ignition. This approach requires studies on high pressure direct injection of light hydrocarbons. In piston engines equipped with a direct injection fuel system the crucial issues influencing the combustion process are: spray atomization and evaporation which strongly depend on the fuel properties, injection pressure and geometry of the injector. These parameters influence the spray process in two main ways, directly and by influencing the phenomena taking place inside the injector. Among the phenomena taking place inside the injector, the fundamental one which strongly influences spray development is cavitation. Due to the fact that light hydrocarbons have higher vapor pressure at a given temperature compared to diesel fuel, they might contribute to the intensification of the cavitation phenomenon inside the injector nozzles. Therefore, in this study special attention was

*Corresponding author

Email addresses: rafal.pyszczek@itc.pw.edu.pl (Rafał Pyszczek), lukasz.kapusta@itc.pw.edu.pl (Łukasz Jan Kapusta), ateod@itc.pw.edu.pl (Andrzej Teodorczyk)

focused on development of the cavitation phenomenon and its impact on the inner nozzle flow parameters. There is experimental evidence which shows that liquid jet atomization near the nozzle exit depends on cavitation [1] and that cavitation probably favors the atomization of the spray [2, 3]. It may, however, induce a mass flow collapse in the internal nozzle flow [4, 5]. Thus, the cavitation phenomenon in fuel injectors can have a positive impact on engine performance and emissions by improving the atomization process as well as a negative impact, by limiting power output through choking the mass flow. Therefore, this phenomenon is of major importance. Although a number of previous works have factored in cavitation and turbulences, the detailed nature of internal nozzle flow is a subject which requires further investigation. In recent years some experimental and numerical studies in this field have been carried out. Most of the recent numerical studies used the Large Eddy Simulation method for this purpose and stated that this method provides sufficient accuracy [4, 6]. Salvador et al. [6] used the LES approach to simulate cavitation in diesel injector nozzles. They validated the code at real operating diesel engine conditions against experimental data with the following parameters: mass flow, momentum flux and effective velocity. They found the CFD code slightly overestimated all of the compared parameters. The deviation of mass flow between the experimental and computational values was around 10%; for velocities it was always lower than 5%. They stated that the code could be considered able to predict the behavior of the flow with a sufficient degree of confidence. Payri et al. [4] conducted a combined experimental and computational study in order to evaluate the ability of the homogeneous multiphase model to predict the behavior of fuel flow and cavitation in the injector nozzles. An extended validation of a code for modelling cavitation was performed in diesel injector nozzles, comparing the CFD results with experimental data and showing a deviation of around 7% between both results. The appearance of cavitation predicted by the numerical simulations showed a cyclical behavior. The continuous changes in vapor distribution had a strong influence on the velocity profile at the exit, and therefore on the air–fuel mixing process in the combustion chamber. Another work of Payri et al. [7] concerned numerical simulations of internal flow in diesel injectors in terms of assessing the capabilities of the LES approach for capturing the turbulent patterns present in the flow. The results were compared to the RANS results and validated against the experimental values and DNS data. Two geometrical models, full geometry of the nozzle and one quarter of the nozzle, were compared. The results showed that the calculations performed on the full geometry model were more accurate. In general, the results showed good agreement with the experimental values and the LES approach turned out to be more accurate than RANS, mainly in the boundary layer. In [8] Payri et al. extended the model with compressibility of the fluid, obtaining even more accurate results. In one of the most recent studies by Ji et al. [9] numerical simulation of the unsteady cavitating turbulent flow around a NACA66 hydrofoil was carried out by means of LES coupled with a homogeneous cavitation model. The predicted cavitation shedding dynamics behavior, including cavity growth, break-off and collapse downstream, agreed fairly well with the experimental observations. The LES results helped to better clarify the physical mechanism for the cavitation induced turbulence and pressure fluctuations. Jollet et al. [10] evaluated several models concerning cavitation. They investigated different combinations of two multiphase models (multifluid and homogeneous model) and two cavitation models (Schnerr-und-Sauer, Zwart-Gerber-Belamri). The results clearly showed the differences between multiphase models, but it is as yet unknown which one of them is nearer to reality. The differences between the two investigated cavitation models were found to be small and the effects of different vapor pressure values were negligible. In the present investigation, after taking into consideration the accuracy of the results from the presented studies, the multifluid approach was chosen, which assumes that two or more phases co-exist at every point in the flow field and each phase is governed by its own set of conservation laws [11].

2. Numerical Model

In recent decades CFD codes have become powerful tools in design processes. It is a branch of fluid mechanics that uses numerical methods and algorithms to solve and analyze problems that involve fluid flows. The most popular method for representing and evaluating partial differential equations in the form of algebraic equations is the finite volume method, in which values are calculated at discrete places on a meshed geometry. “Finite volume” refers to the small volume surrounding each node point on a mesh. One of the solvers based on that method is AVL Fire, which was used for the numerical simulations presented in this paper.

2.1. Turbulence

Experimental study of the turbulence developed within injector nozzles and its interaction with the cavitation phenomenon presents huge difficulties due to the extremely small size of the holes, the existence of a multiphase flow and high velocities. Therefore, the Large Eddy Simulation method has become a great alternative to simulate internal flow. Researchers who used the LES method in their numerical studies of cavitation in fuel injectors have stated that this method provides sufficient accuracy [4,6]. Therefore, LES was chosen for this investigation. LES is based on capturing the large scale motions of the flow and modelling the scale motions smaller than the mesh spacing. It is a compromise between Direct Numerical Simulation (DNS) which is currently unavailable in commercial use and Reynolds Averaged Navier–Stokes (RANS), the method of the lowest computational resources demands. In the LES approach, the equations describing the flow are spatially filtered using a filter function. Large scale motions, such as movement and interactions between large eddies, are calculated directly from Navier-Stokes equations. In contrast, the small scale motions and the influence of small eddies on the large ones

are modelled. The filtering operation can be defined as follows [12]:

$$\overline{\phi(x,t)} = \int_{-\infty}^{\infty}\int_{-\infty}^{\infty}\phi(r,t')G(x-r,t-t')dt'dr \tag{1}$$

where G is a convolution kernel unique to the filter type used and ϕ is the filtered parameter. The most popular filter functions are Gaussian, Ideal Low Pass Filter and Box Filter, as described in [13] and [14]. In general, the filter coefficient depends on the size of the mesh elements. Once the filtering operation (1) is applied to the governing equations, the filtered equations of the motion are obtained. For turbulent structures bigger than the mesh, these equations are solved directly and govern the evolution of the large, energy-carrying scales of motion [15]:

$$\frac{\partial\overline{u}_i}{\partial x_i} = 0 \tag{2}$$

$$\frac{\partial\overline{u}_i}{\partial t} + \frac{\partial}{\partial x_j}(\overline{u}_i\overline{u}_j) = -\frac{1}{\rho}\frac{\partial\overline{p}}{\partial x_i} - \frac{\partial\tau_i j}{\partial x_j} + \nu\frac{\partial^2\overline{u}_i}{\partial x_i\partial x_j} \tag{3}$$

Structures smaller than the mesh spacing are taken into account by defining subgrid-scale (SGS) velocity $u_i' = u_i - \overline{u_i}$ and introducing a subgrid-scale (SGS) stress term [15]:

$$\tau_{ij} = \overline{u_iu_j} - \overline{u}_i\overline{u}_j = L_{ij} + C_{ij} + R_{ij} \tag{4}$$

where: $L_{ij} = \overline{\overline{u}_i\overline{u}_i} - \overline{u}_i\overline{u}_i$ are the Leonard stresses, $C_{ij} = \overline{\overline{u}_iu_j'} + \overline{u_i'\overline{u}_j}$ are the cross terms and $R_{ij} = \overline{u_i'u_j'}$ are the SGS Reynolds stresses.

The Leonard stresses represent interactions between resolved scales that result in subgrid-scale contributions, the cross terms represent interactions between resolved and unresolved scales, and the SGS Reynolds stresses represent interactions between small, unresolved scales. In the LES method, the dissipative scales of motion smaller than the mesh spacing are resolved poorly or not at all. Therefore, a SGS model is needed to account for these scales. The role of the SGS model is very important, because the subgrid scale stress contains 20% of the flow turbulence kinetic energy. Over the years, several SGS models have been developed [16, 17]. Most of them are eddy-viscosity models of the form [15]:

$$\tau_{ij} = -\frac{\delta_{ij}}{3}\tau_{kk} = -2\nu_T\overline{S}_{ij} \tag{5}$$

where $\overline{S}_{ij}$ is the large-scale strain-rate tensor:

$$\overline{S}_{ij} = \frac{1}{2}\left(\frac{\partial\overline{u}_i}{\partial x_j} + \frac{\partial\overline{u}_j}{\partial x_i}\right) \tag{6}$$

The SGS model used in this study was the Smagorinsky model [18]. Although recently more advanced SGS models have been developed and used for turbulence modeling [9], the Smagorinsky model is still one of the most convenient and widely used models for channels and internal flows [7]. This particular model was also used in recent works [6, 8] for LES numerical modeling of cavitation and its interaction with the turbulence developed in diesel injector nozzles. Therefore it should also be suitable for this study. The eddy viscosity in the Smagorinsky SGS model is defined as [15]:

$$\nu_T = C\Delta^2\sqrt{2\overline{S}_{ij}\overline{S}_{ij}} \tag{7}$$

where: Δ is the grid size and C is the model constant.

The most important advantage of the LES method is a significant computational cost reduction compared to the DNS method, which according to [19] can be estimated as:

$$N_{\mathrm{LES}} + \left(\frac{0.4}{Re^{0.25}}\right)N_{\mathrm{DNS}} \tag{8}$$

In combination with much higher accuracy than the RANS model results, the LES became a real alternative to simulate internal flow in commercial applications.

2.2. Cavitation

Two-phase flow through the injector nozzle with liquid fuel as the continuous phase and fuel vapor as the dispersed phase is one of the basic cases of multiphase flows. This type of the flow requires modeling, using the most general approach called *Euler–Euler*. In this approach, the different phases are treated mathematically as interpenetrating continua. Since the volume of a phase cannot be occupied by another phase, the concept of volume fraction is introduced. The volume fractions of each phase are assumed to be a continuous function of space and time, and their sum is equal to one. The conservation equations for each phase are derived to obtain a set of equations, which have a similar structure for all phases [20]. The cavitation is modeled by including source terms of mass, momentum and energy exchange in the conservation equations. The liquid-vapor mass transfer (evaporation and condensation) is governed by the vapor transport equation [21]:

$$\frac{\partial}{\partial t}(\alpha_v\rho_v) + \nabla\cdot(\alpha_v\rho_v\vec{v_v}) = R_e - R_c \tag{9}$$

where: α_v refers to the volume fraction of the vapor phase, ρ_v is the density of the vapors phase, $\vec{v_v}$ the velocity of the vapor phase, R_e and R_c describe the mass transfer related to the vapor bubbles expansion and collapse.

In the cavitation model, one must assume that there are plenty of nuclei for the inception of cavitation. Thus, the primary focus is on proper accounting of bubble growth and collapse. The bubble dynamics equation can be derived from the generalized Rayleigh–Plesset equation [22]:

$$R_B\frac{d^2R_B}{dt^2} + \frac{3}{2}\left(\frac{dR_B}{dt}\right)^2 = \left(\frac{P_B - P}{\rho_l}\right) - \frac{4\nu_l}{R_B}\frac{dR_B}{dt} - \frac{2\sigma}{\rho_l R_B} \tag{10}$$

where R_B is the bubble radius, σ is the liquid surface tension, ρ_l is the liquid density, P_B is the bubble surface pressure, P is the local far-field pressure, ν_l is the liquid kinematic viscosity.

The simulations presented in this paper were done using the multifluid model, which requires by default the calculation of the complete set of the conservation equations and volume fraction equation for each phase representing the basis of Euler-Euler approach in modeling the multiphase flows. As for the cavitation phenomenon model used in this study, it was based on a simplified version of Rayleigh-Plesset equation, where viscosity, surface tension forces and bubble interaction are neglected [23].

$$R_B \frac{d^2 R_B}{dt^2} + \frac{3}{2}\left(\frac{dR_B}{dt}\right)^2 = \left(\frac{P_{sat} - P}{\rho_l}\right) - \frac{2}{3} C_E k_l \qquad (11)$$

where k_l is the turbulent kinetic energy of the liquid phase and C_E is the Egler coefficient which depends on the local turbulence level [20].

2.3. Boundary conditions and computational mesh

Table 1: Parameters of investigated cases

Investigated fuel	n-hexane
Nozzle diameter, mm	0.65
Number of nozzles	3
Injection duration	18°CA (4 ms)
Needle lift, mm	1.85
Investigated fuel pressure, MPa	35, 50, 65
Investigated backpressure, MPa	6.5, 9.3, 11.0

The injector under investigation and presented in this paper consists of three cylindrical nozzles, each with a diameter of 0.65 mm. Its unique design is an initial requirement and derives from its location in the chamber, which is not the subject of this study. For numerical simulations the entire domain was taken into consideration, even though the symmetrical shape of the injector permitted the use of only half of the injector interior. This was done in order to avoid symmetry plane going through the nozzle, which could restrict the growth of any large eddy [7]. Payri et al. [7], when simulating cavitation in the injector nozzle, stated clearly that it is with for full geometry of the nozzle that the LES methodology works properly and typical turbulent structures are generated. The whole injection process and movement of the needle last 18° of crankshaft angle at specified engine speed of 750 rpm. During the first 2° the needle was opening and during the last 2° it was closing. The maximum lift of the needle was 1.85 mm. Hexane was selected as the fluid flowing through the injector due to the fact that it is a constituent of natural gas condensate which stays liquid in ambient conditions. The temperature was set at 315 K and fluid properties such as liquid density ρ_l, gaseous density ρ_g, liquid dynamic viscosity μ_l, gaseous dynamic viscosityμ_g and saturation pressurep_{sat} were taken from [23] and entered in the solver settings. Three different fuel pressures at the inlet (35 MPa, 50 MPa, 65 MPa) and three different backpressures at the outlet (11 MPa, 9.3 MPa, 6.5 MPa) were under investigation. In order to best reflect real conditions, the initial conditions were introduced as follows: the volume of the injector above the needle tip filled with the fuel of pressure equal to the inlet pressure, the volume below the needle tip together with nozzles filled with fuel of pressure equal to the backpressure. Due to the low number of test variables and levels of each variable, the classical factorial approach, where each variable is tested at every level of the other variables, was used to select the cases for the investigation. This approach led to a total number of 9 investigated cases. A summary of the considered parameters is given in Table 1.

A number of numerical studies done in the area of cavitating flows in fuel injectors applied two different approaches to defining the outlet boundary condition. In the first one, the outlet boundary condition is applied directly on the nozzle outlet [4, 6, 24–27]. In the second one, additional volumes are attached to the nozzle outlets and the outlet boundary condition is located on the external surfaces of the attached volumes [28–31].

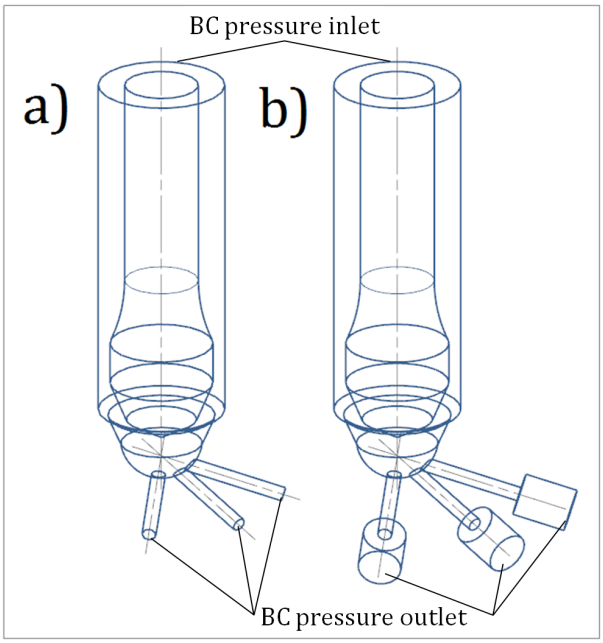

Figure 1: Two different models with applied boundary conditions; a) simple model; b)extended model

In this study, both approaches were analyzed in order to investigate the influence of the additional volume at the nozzle flow. For this purpose two models were prepared – simple one and extended one with additional discharge volumes at the outlet of the nozzles (Fig. 1). In both of them the pressure boundary condition was applied at the inlet of the injector. In the simple model the pressure outlet boundary condition was applied at the outlets of the nozzles. In the model with attached volumes the pressure outlet boundary condition was applied at the external surfaces of the additional volumes. The calculations were initialized with volumes filled with air of pressure equal to the backpressure, while the rest of the domain was initialized in the same way as for the simple model. Thanks to this approach, in the cases where gaseous phase was present at the outlets of the nozzles, it could condense

in the additional volumes and did not reach the outlets. It improved the solution convergence and reduced numerical oscillations in cases where gaseous phase reached the pressure outlet boundary condition. A similar solution for numerical investigations was recommended by He et al. [28, 29]. They concluded that when the surrounding pressure boundary condition is used directly on the exit of the nozzle, the accuracy of the calculation results may be affected [29].

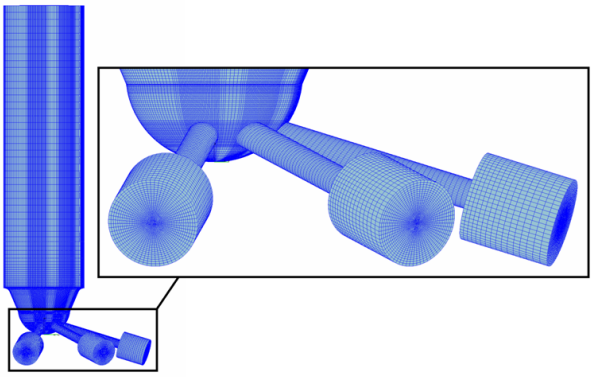

Figure 2: Extended model mesh used for simulations

The mesh used for the simulations presented in this study consisted of ten moving layers between the needle tip and the needle seat, in order to simulate the movement of the needle and determine its influence on the flow. For the model with additional volumes, the mesh consisted of 828408 elements and is presented in Fig. 2. For the simple model, the mesh comprised 741432 elements and lacked the discharge volumes. The smallest element sizing was inside the nozzles and was of 0.02 mm. The number of mesh elements was restricted by the available computational resources. Assuming that integral turbulence length scales inside the nozzle would be the order of magnitude of the turbulent scales in the fully developed duct flow, which is 0.07 of the hydraulic diameter, the biggest expected scales in the investigated cases are to be 0.07×0.65 mm = 0.046 mm. Therefore, these scales can be resolved directly on the described mesh by LES. However, the turbulence induced by the cavitation bubbles growth and collapse is expected to be of much smaller scales and will be resolved by the SGS model.

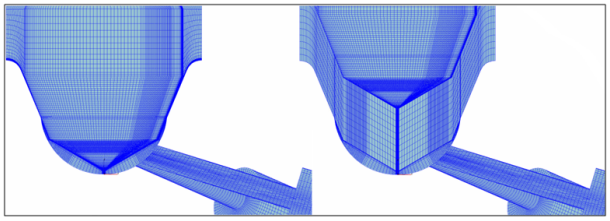

Figure 3: Extreme positions of the needle; left – fully closed, right – fully open

A section through the injector mesh showing the needle in extreme positions is presented in Fig. 3.

3. Results

3.1. Mesh comparison

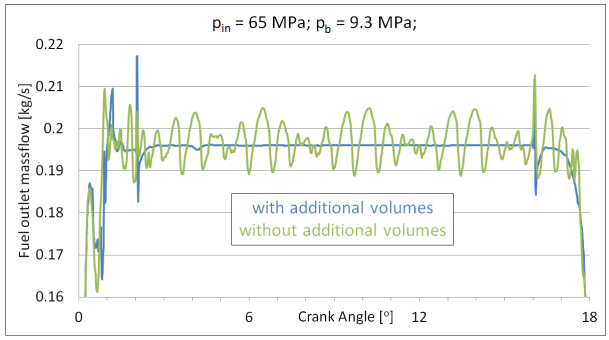

Figure 4: Fuel mass flow results obtained with two different models where p_{in}=65 MPa and p_b=9.3 MPa

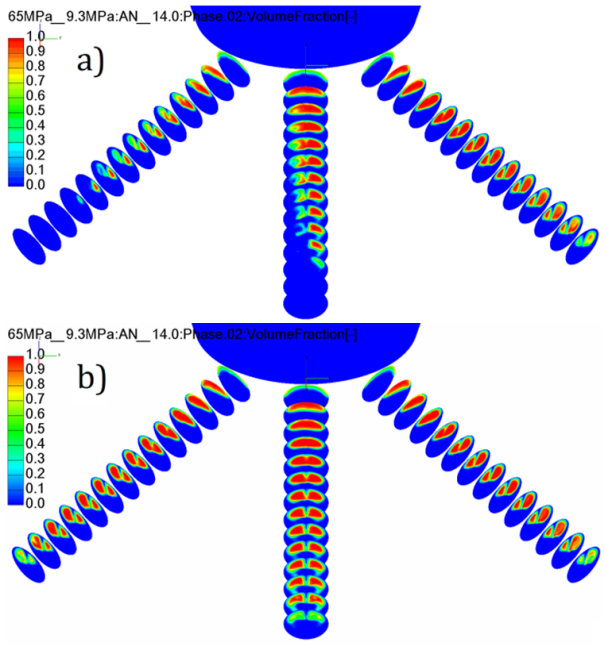

Figure 5: Gaseous phase distribution for case p_{in}=65 MPa and p_b=9.3 MPa and two different models; a) without b) with volumes at the outlet

The comparison of the hexane mass flow at the outlet of the nozzles for two different models and the case where the fuel pressure p_{in} was of 65 MPa and the backpressure p_b was of 9.3 MPa is presented in Fig. 4. Although the average value of the fuel mass flow during the full injection process was the same, the results obtained with the simple model showed strong fluctuations of the flow parameters. This is due to the fact that in this case the gaseous phase reached the outlet of the nozzles and surfaces with specified pressure outlet boundary condition (Fig. 5). Interestingly, these fluctuations were observed in only two of the three nozzles, which is hard to explain and might be just due to the geometrical parameters of the injector. The difference between the nozzles in the gaseous phase distribution is shown in Fig. 5.

The results obtained using two different models confirm that application of the discharge volume provides a more realistic outlet boundary condition, improves solution convergence and reduces numerical oscillations in cases where the gaseous phase reaches the pressure outlet boundary condition. Hence, the model with discharge volumes at the outlet of the nozzles was chosen for simulations of all the investigated cases.

3.2. In-injector cavitation

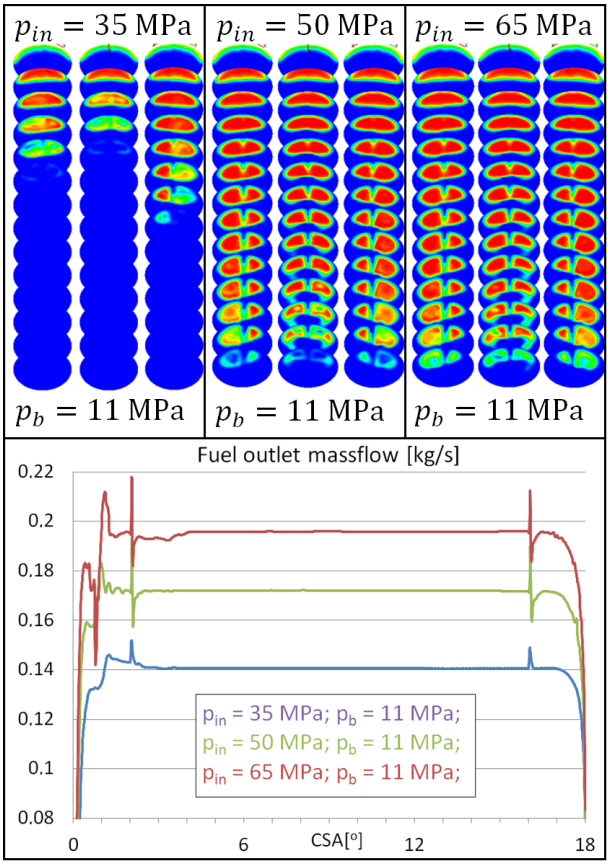

Figure 6: Vapor phase distribution for each nozzle (left, central and right), for different injection pressure and for backpressure of 11MPa and graph presenting corresponding fuel mass flow at the outlets

In this section, the detailed results of the gaseous phase distribution and fuel mass flow are presented. The vapor phase distribution results shown in Fig. 6, 7 and 8 represent the moment when the needle was fully opened and the flow was steady, which provides an opportunity to compare these results between the cases and the nozzles in each case. Furthermore, the averaged results of the hexane mass flow, gaseous phase volume fraction and gaseous phase outlet mass flow are presented in order to show the influence of the fuel pressure and backpressure on the mass flow and cavitation intensity.

The mass flow at the outlet versus the needle lift graphs presented in Fig. 6, 7 clearly show that the movement of the needle strongly affects the flow, especially in the opening

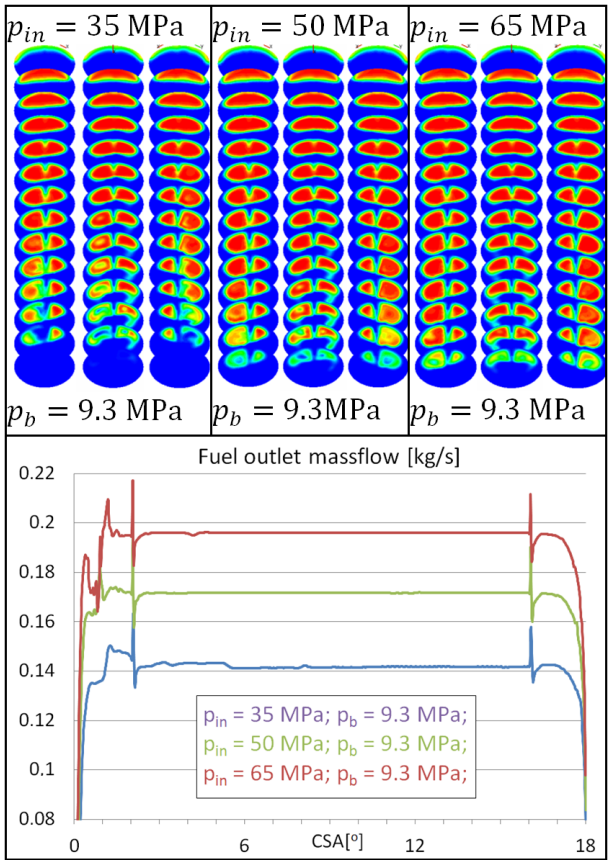

Figure 7: Vapor phase distribution for each nozzle (left, central and right) for different injection pressure and for backpressure of 9.3MPa and graph presenting corresponding fuel mass flow at the outlets

stage. The hexane mass flow reaches the maximum value after about 1^o in every case. At this point the needle is still being lifted, but the mass flow is limited by the pressure difference and the area of the cross-sections of the nozzles. Until 2^o strong fluctuations of the mass flow can be observed. When the needle reaches the maximum lift, the mass flow becomes steady. At 16^o, the process of the injector closing starts. The fuel mass flow is maintained constant until around 17^o and after that it collapses rapidly. The closing process proceeds mildly, without any strong fluctuations, unlike the opening process.

The results differ between the nozzles. This is caused by the asymmetrical arrangement of the nozzles. The vapor phase in each nozzle is clearly divided into two cores, which was also observed by other authors [6, 32]. This kind of behavior could be related to the turbulence present in the flow.

The results presented in Fig. 9. clearly show that the highest values of turbulence energy can be seen at the inlet and at the outlet of the nozzles - the places of growth and collapse of the vapor bubbles. Furthermore, if the vapor phase within the nozzle is compared to the vorticity (Fig. 9.), it can be stated that the highest values of vorticity occur where the vapor bubbles grow, reach maximum values at the interphase region and collapse. Similar conclusions about in-

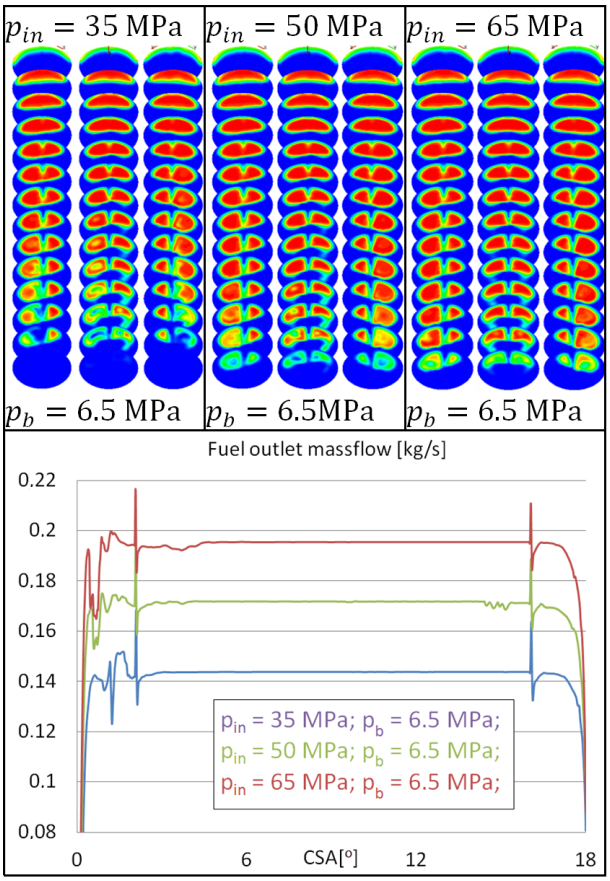

Figure 8: Vapor phase distribution for each nozzle (left, central and right) for different injection pressure and for backpressure of 6.5MPa and graph presenting corresponding fuel mass flow at the outlets

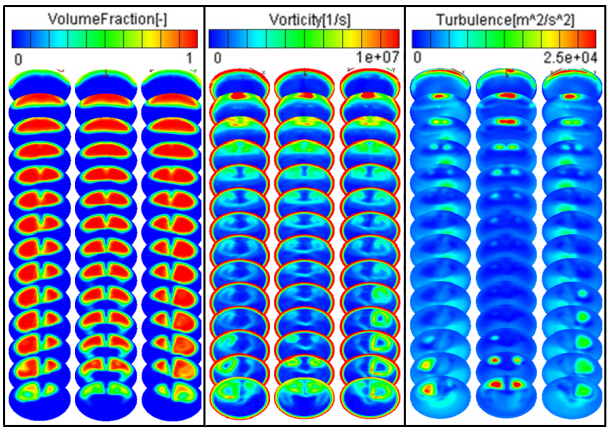

Figure 9: Vapor phase distribution (a), vorticity (b) and total turbulence energy (c) for each nozzle for case p_{in}=65MPa and p_b=9.3MPa

teraction between cavitation and turbulence were presented in [6].

In Fig. 10 and 11 the averaged results of the hexane mass flow for all cases are compared in order to verify the influence of fuel pressure and backpressure on mass flow. It transpires that the hexane outlet mass flow mostly depends on the fuel pressure. The influence of backpressure on this parameter

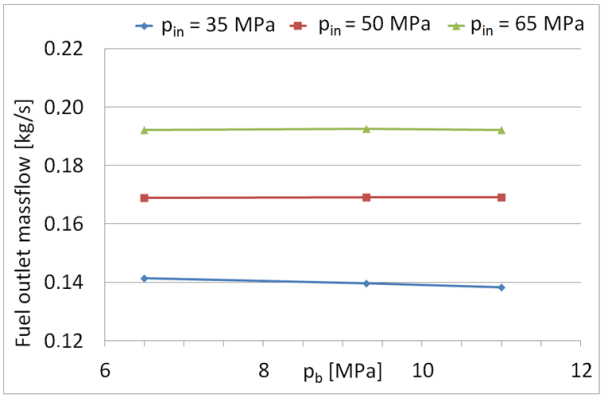

Figure 10: The influence of backpressure on fuel outlet mass flow

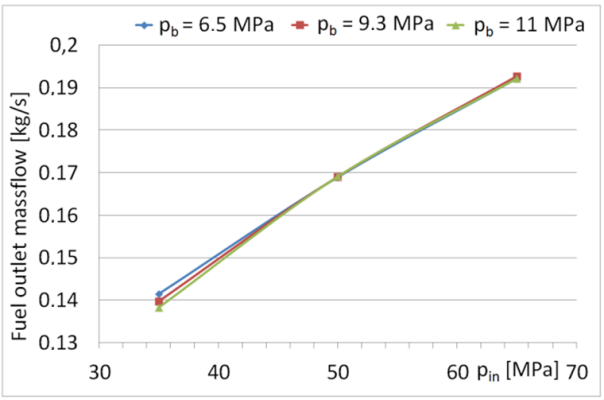

Figure 11: The influence of injection pressure on fuel outlet mass flow

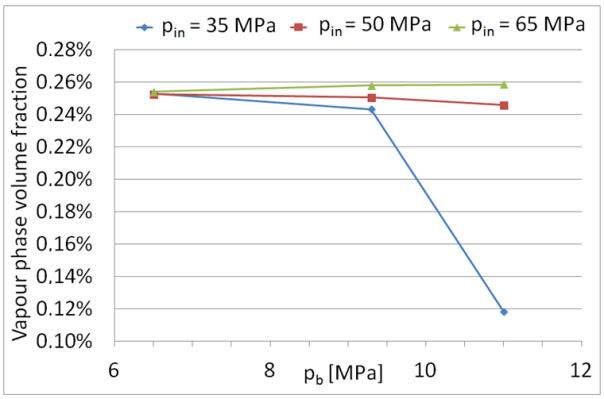

Figure 12: The influence of backpressure on the vapor phase volume fraction

in conditions which were under investigation in this study is negligible. In Fig. 12 and 13 the average values of gaseous phase volume fraction are presented. The results are at the same level of 0.24–0.26% for eight of nine cases. Only in the case where the injection pressure p_in was 35 MPa and the backpressurep_b was 11 MPa did the vapor phase volume fraction reach the level of 0.12%. This means that for the investigated conditions the intensity of cavitation was not affected by either the fuel pressure or the backpressure except in one case, where the pressure difference between the

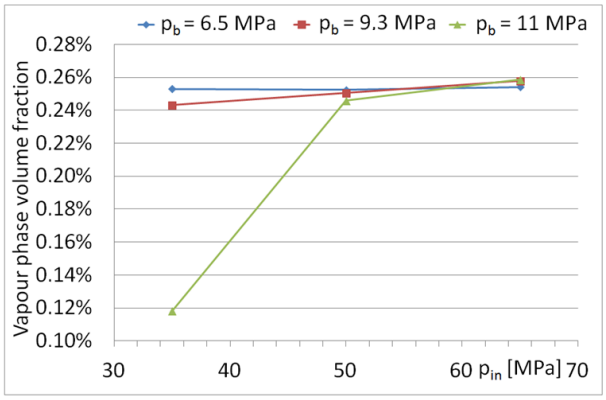

Figure 13: The influence of injection pressure on the vapor phase volume fraction

inlet and the outlet had a minimal value. This one case indicates that the intensity of cavitation will decrease with the decrease in the difference between inlet and outlet pressure.

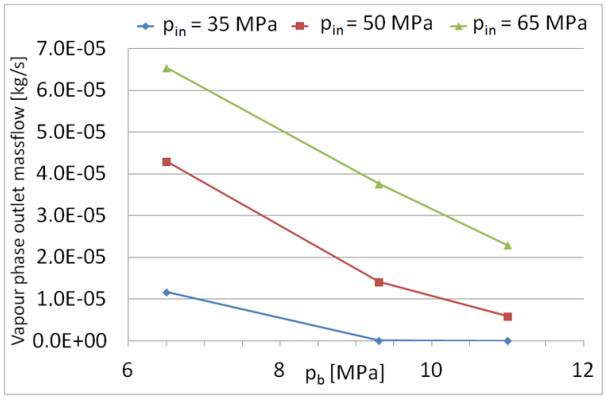

Figure 14: The influence of backpressure on the vapor phase mass flow

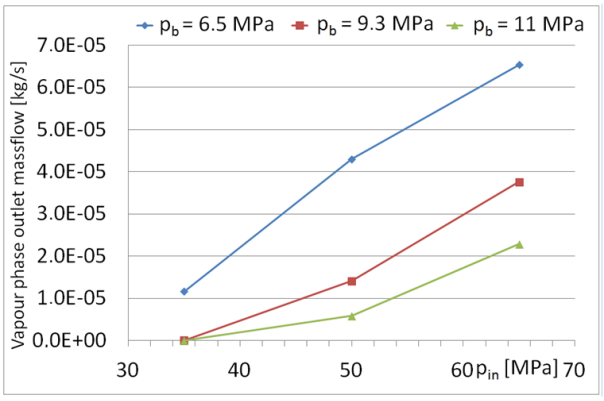

Figure 15: The influence of injection pressure on the vapor phase mass flow

Although the vapor phase volume fraction is almost the same in all cases, its mass flow at the outlet varies, as is shown in Fig. 14 and 15. Only in two cases where the fuel pressure at the inlet p_{in} was 35 MPa and the backpressure p_b was 11 MPa and 9.3 MPa does the gaseous phase not reach the outlet of the nozzles. In all of the other seven cases it reaches the outlet with different intensity, depending strongly on both fuel pressure and backpressure.

4. Conclusion

A total of nine simulations for three different hexane pressures and three different backpressures were conducted. The results were presented to show the influence of pressure and backpressure on fuel flow. The LES model was used to track flow turbulence and its interaction with cavitation. Two approaches to defining outlet boundary condition were investigated. In the first one, the outlet boundary condition was applied directly on the nozzle outlet. In the second one, additional volumes were attached to the nozzle outlets and the outlet boundary condition was located on the external surfaces of the attached volume. Based on the results obtained, the following conclusions were made:

- The additional volumes at the outlets improved the convergence of the simulations. These volumes let the vapor phase condense after exiting the nozzles, so the vapor phase did not reach the outlet with the specified pressure outlet boundary condition.
- The fuel outlet mass flow was dependent on the inlet pressure, backpressure and position of the needle.
- The inlet pressure had the biggest influence on the maximum fuel mass flow, but the influence of backpressure on fuel mass flow under investigated conditions was negligible.
- The presence of the vapor phase at the exit of the nozzles did not affect average fuel mass flow.
- The maximum mass flow was reached at about half of the needle lift, which means that a lift as high as 1.85 mm is not necessary and can be reduced to about 1 mm without decreasing the mass flow.
- The vapor phase volume fraction and the mass flow at the outlet was dependent on both fuel pressure and backpressure. More vapor can be observed at the exit of the nozzles, when fuel pressure increases and backpressure decreases. It is related to the differences in fuel velocity in the nozzles caused by pressure differences.
- Interaction between cavitation and turbulence is observed in the flow through the injector nozzles. Turbulence is enhanced by cavitation, since the highest values of vorticity and turbulence energy are found in regions of growth and collapse of vapor bubbles and at the liquid-vapor interphase.

Acknowledgments

This study was funded by the National Science Center of Poland within the framework of the OPUS programme under agreement UMO-2012/07/B/ST8/03632.

The Fire calculation code was used as per the AVL AST University Partnership Program. The authors would also like to acknowledge Ms Klaudyna Banaszek for her proof reading service.

References

[1] A. Sou, S. Hosokawa, A. Tomiyama, Effects of cavitation in a nozzle on liquid jet atomization, Int. J. Heat Mass Transfer 50 (2007) 3575–3582.
[2] F. Payri, V. Bermudez, R. Payri, F. Salvador, The influence of cavitation on the internal flow and the spray characteristics in diesel injection nozzles, Fuel 83 (2004) 419–431.
[3] R. Payri, J. Garcia, F. Salvador, J. Gimeno, Using spray momentum flux measurements to understand the influence of diesel nozzle geometry on spray characteristics, Fuel 84 (2005) 551–561.
[4] F. Payri, R. Payri, F. Salvador, J. Martínez-López, A contribution to the understanding of cavitation effects in diesel injector nozzles through a combined experimental and computational investigation, Comput Fluids 58 (2012) 88–101.
[5] J. Javier López, F. Salvador, O. de la Garza, J. Arrègle, A comprehensive study on the effect of cavitation on injection velocity in diesel nozzles, Energy Conversion and Management 64 (2012) 415–423.
[6] F. Salvador, J. Martínez-López, J.-V. Romero, M.-D. Roselló, Computational study of the cavitation phenomenon and its interaction with the turbulence developed in diesel injector nozzles by large eddy simulation (les), Math Comput Modell 57 (2013) 1656–1662.
[7] R. Payri, B. Tormos, J. Gimeno, G. Bracho, The potential of large eddy simulation (les) code for the modeling of flow in diesel injectors, Math Comput Modell 2010 (2010) 1151–1160.
[8] R. Payri, B. Tormos, J. Gimeno, G. Bracho, Large eddy simulation for high pressure flows: Model extension for compressible liquids, Math Comput Modell 54 (2011) 1725–1731.
[9] B. Ji, X. Luo, R. Arndt, X. Peng, Y. Wu, Large eddy simulation and theoretical investigations of the transient cavitating vortical flow structure around a naca66 hydrofoil, Int J Multiphase Flow 68 (2015) 121–134.
[10] S. Jollet, T. Willeke, F. Dinkelacker, Comparison of various models for transient nozzle flow simulations including time-resolved needle lift, in: 12th Trienn. Int. Conf. Liq. At. Spray Syst., vol. i, Heidelberg, Germany, 2012, pp. 1–8.
[11] E. Goncalves, R. Patella, Numerical simulation of cavitating flows with homogeneous models, Comput Fluids 38 (2009) 1682–1696.
[12] P. Sagaut, Large Eddy Simulation for Incompressible Flows, 3rd Edition, Springer, 2006.
[13] L. Berselli, T. Iliescu, W. Layton, Mathematics of Large Eddy Simulation of Turbulent Flows, Springer, 2005.
[14] T. Iliescu, Large eddy simulation for turbulent flows, Ph.D. thesis (2000).
[15] U. Piomelli, Large-eddy simulation: achievements and challenges, Prog Aerosp Sci 35 (1999) 335–362.
[16] J. McDonough, ntroductory lectures on turbulence physics, mathematics and modeling, Departments of Mechanical Engineering and Mathematics, University of Kentucky (2004).
[17] P. Jaworski, M. Żbikowski, Modele les w badaniach numerycznych procesów spalania w silnikach tłokowych - przegląd literatury (in polish), Arch Comb 11 (2011) 111–144.
[18] J. Smagorinsky, General circulation experiments with the primitive equations, Mon Weather Rev 91 (1963) 99–164.
[19] D. Wilcox, Turbulence modeling for CFD, DCW Industries, Inc, 1998.
[20] A. L. GmbH, Eulerian multiphase. avl fire softw doc. (2013).
[21] H. El-Din, Y.-S. Zhang, M. Elkelawy, A computational study of cavitation model validity using a new quantitative criterion, Chinese Phys Lett 29.
[22] C. Brennen, Cavitation and bubble dynamics, Oxford University Press, 1995.
[23] N. C. WebBook, [Online] Available: http://webbook.nist.gov/chemistry/. [Accessed: 06-Jun-2013].
[24] F. Salvador, J.-V. Romero, M.-D. Roselló, J. Martínez-López, Validation of a code for modeling cavitation phenomena in diesel injector nozzles, Math Comput Model 52 (2010) 1123–1132.
[25] F. Salvador, J. Martínez-López, Study of the influence of the needle lift on the internal flow and cavitation phenomenon in diesel injector nozzles by cfd using rans methods, Energy Convers Manag 66 (2013) 246–256.
[26] F. Salvador, J. Martínez-López, J.-V. Romero, M.-D. Roselló, Influence of biofuels on the internal flow in diesel injector nozzles, Math Comput Model 54 (2011) 1699–1705.
[27] X. Wang, K. Li, W. Su, Experimental and numerical investigations on internal flow characteristics of diesel nozzle under real fuel injection conditions, Exp Therm Fluid Sci 42 (2012) 204–211.
[28] Z. He, W. Zhong, Q. Wang, Z. Jiang, Y. Fu, An investigation of transient nature of the cavitating flow in injector nozzles, Appl Therm Eng.
[29] Z. He, W. Zhong, Q. Wang, Z. Jiang, Z. Shao, Effect of nozzle geometrical and dynamic factors on cavitating and turbulent flow in a diesel multi-hole injector nozzle, Int J Therm Sci 70 (2013) 132–143.
[30] M. Jia, M. Xie, H. Liu, W.-H. Lam, T. Wang, Numerical simulation of cavitation in the conical-spray nozzle for diesel premixed charge compression ignition engines, Fuel 90 (2011) 2652–2661.
[31] S. Gopalakrishnan, D. Schmidt, A computational study of flashing flow in fuel injector nozzles, SAE Int J Engines (2009) 160–170.
[32] Y. Melsem, S. Honnet, W. Schwarz, J. Reveillon, F. Demoulin, Modeling of cavitating flows in diesel injector nozzles to consider its impact on the atomization, in: 24th Eur. Conf. Liq. At. Spray Syst., 2011, estoril, Portugal.